Propagation of hydroelastic waves in a thin ice sheet

Vasco Zanchi
Université Paris Cité
Advisors : Antonin Eddi, Stéphane Perrard
Laboratory : PMMH (ESPCI)

August 31, 2024

Figure 1: Photography of ice floes taken in 2023 in Rimouski (Canada) by our team. The region separating the water and the continuous ice, where we can see broken ice floes of different sizes, is called the marginal ice zone.

Contents

1 Introduction **3**
- 1.1 Context . . . 3
- 1.2 Hydroelastic waves . . . 3
- 1.3 Scientific Question . . . 3

2 Theoretical framework **3**
- 2.1 Model . . . 3
- 2.2 Characteristic wavelengths in the experiment . . . 5

3 Numerical tools **6**
- 3.1 PIV (particle image velocimetry) . . . 6
  - 3.1.1 Explaination using synthetic images . . . 6
  - 3.1.2 PIV algorithm in practice . . . 6
  - 3.1.3 Conversion of coordinates and distances from pixels to windows units . . . 7
  - 3.1.4 Maximization of the PIV efficiency . . . 8
- 3.2 Fourier transforms . . . 8
  - 3.2.1 Continuous case . . . 8
  - 3.2.2 Discrete case . . . 9
  - 3.2.3 The use of Fourier transforms for wave dispersion relations . . . 9
- 3.3 A combination of stroboscopic measurements and Fourier analysis . . . 10
  - 3.3.1 Stroboscopy . . . 10
  - 3.3.2 How to extract quickly the component of the signal at a given frequency . . . 11
  - 3.3.3 Combination of the two methods . . . 11

4 Experiments **12**
- 4.1 Experimental setup . . . 12
- 4.2 Testing the experimental setup with a known material . . . 14
- 4.3 A first experiment to put in evidence ice heterogeneity . . . 16
- 4.4 A second data set on ice to measure a dispersion relation . . . 19
  - 4.4.1 Set up . . . 19
  - 4.4.2 Measure of the horizontal aspect ratio as a function of the position on the image 19
  - 4.4.3 PIV analysis, and filtering of the data . . . 21
  - 4.4.4 Resulting dispersion relation . . . 23

5 Conclusion **24**

6 Appendix **26**
- 6.1 Code for Fig.5 . . . 26

1 Introduction

1.1 Context

Due to global warming, sea ice properties have been rapidly changing in the last decades. Some properties of scientific interest are the area covered by the ice floes, the dimensions of the ice floes, but also the mechanical properties of the ice. Several phenomena are in play. Some important processes are the melting of the ice floes or the solidification of water. But these are not the only processes : fracture mechanisms of ice floes have to be considered as well. In 2006, an important work has been published [TTN06], in which the distribution of sizes of sea ice floes has been measured on the field for a range of about 4 decades of ice floe diameter sizes. This distribution has put in evidence the existence of two distinct regimes : small ice floes (from about 1 meter to about 40 meters of diameter) seem to fracture in a different way than big ice floes (from about 40 meters to about 1000 meters of diameter). Still today, the origins of these two different behaviours are not well understood. The direction taken by our experimental team is to investigate the coupling between ocean waves and the ice floes. To do so, the team has already made field measurements in Canada (Fig.1), and has performed lab experiments with other floating materials than ice. This internship is the first work in our team in which we study real ice in the lab.

1.2 Hydroelastic waves

The study of the coupling between water waves and ice floes is a way to measure ice mechanical properties. To study this coupling, one method, as we do in this report, is to model sea ice as a floating elastic plate, and measure the dispersion relation of surface waves, i.e. the waves that propagate in a thin elastic solid. In elastic plates, 3 types of waves are relevant for our problem. The first ones are the shear-horizontal waves, characterized by displacements parallel to the surface and perpendicular to the propagation. The second ones are the longitudinal waves : they compress and dilate locally the solid. These ones are analogous to acoustic waves in gases for instance. The third ones are associated to the vertical motion of the sea ice : they are called hydroelastic waves. We focus here on this last type of waves, that correspond somehow to the coupling between gravity-capillary waves and the waves associated to the vertical motion of a thin elastic plate.

1.3 Scientific Question

In a floating ice sheet at the lab scale, due to the difficulties to obtain a perfectly homogeneous surface, it is not evident that hydroelastic waves can propagate in an ice sheet grown in the lab. Therefore, the main question that we address in this report is : can we measure a dispersion relation in a heterogenous ice sheet grown in the lab? To approach the problem, we first had to find an efficient way to grow an ice sheet in the lab, and then to measure local displacements on it, with a method that is convenient and accurate, not only in the lab, but also potentially on the field. To measure the propagation of waves in the ice, one can use geophones, as it has been proposed in the nineties [SEP98], which is convenient for field experiments, when the sea ice is thick enough. In the lab, if we want to observe phenomena equivalent to the ones on the field, the ice sheet has to be from 100 to 1000 times smaller than sea ice on the field. Therefore, the technique that we have used is rather based on optical acquisitions than mechanical measurements. It can turn out to be useful even on the field, when the ice thickness is too small to probe locally the mechanics of the material.

In this report, we will first present the theoretical framework, to explain how we model the ice sheet. Then we will talk about the numerical tools, used to process our experimental data. Eventually we will present some experiments, and the main experimental results that we have obtained.

2 Theoretical framework

2.1 Model

To understand the propagation of waves in an ice sheet covering the surface of water, we model the ice sheet by an elastic plate. The thickness of the plate is noted h. Its density is written ρ. It has a Young modulus E and a Poisson ratio ν. The water has a finite depth H below the plate. In this model, 3

mechanisms govern the propagation of waves. The first one is the gravitational force applied to the water : since each fluid particle is submitted to the acceleration of gravity g, Archimedes force plays the role of restoring force that tends to bring the fluid back to its equilibrium position. The second mechanism is tension : the corresponding restoring force is due to the longitudinal compression, or dilatation of the elastic plate. The mechanical tension T, related to the mechanical stress σ with the relation $\sigma = \frac{T}{h}$. The tension is related to capillary forces from the surface of water as well, because modifying locally the surface of the sheet that is in contact with water requires an additional energetic cost. The third mechanism is flexion : the corresponding restoring force is due to the application of a curvature to the elastic plate. To this third mechanism, the associated parameter is the flexural modulus D.

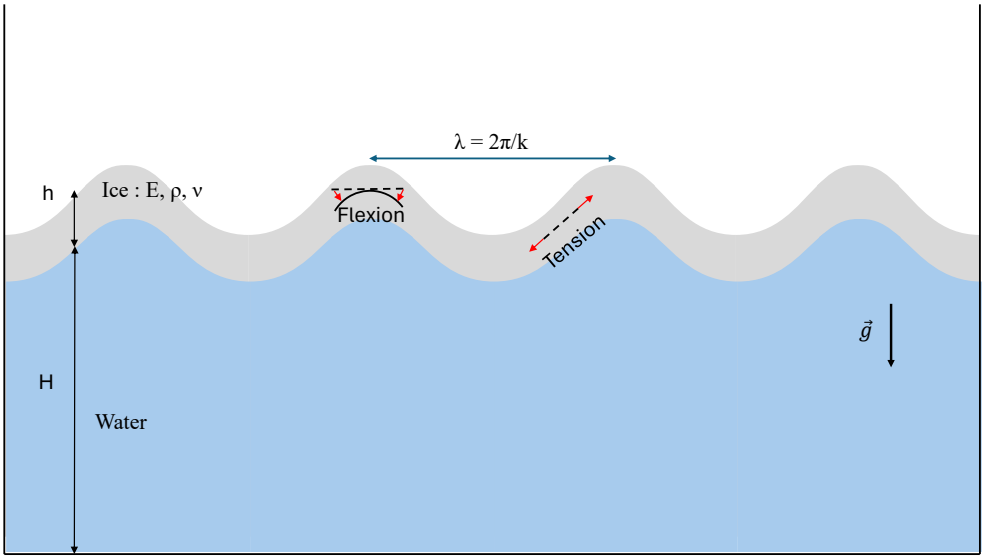

Figure 2: Sketch of a thin elastic sheet covering the surface of water. It has a Young modulus E, a Poisson ratio ν, and a density ρ. In this example, a sinusoidal wave with wavelength $\lambda = \frac{2\pi}{k}$ is propagating along the horizontal axis

Under the hypotheses that :

- displacements are small so that we stay in the linear regime.
- We look for hydroelastic waves, that correspond to motion only along the vertical axis.
- inertia of the elastic sheet is negligible : that corresponds to an infinitely thin sheet ($kh << 1$)
- the fluid below is a perfect fluid : it has no viscosity
- the fluid is incompressible : the sound speed in water is much higher than all other phase velocities that are in play in the problem.

The dispersion relation of hydroelastic waves in our system is given by the following equation [Dom18]:

$$\omega^2 = (gk + \frac{T}{\rho}k^3 + \frac{D}{\rho}k^5) \cdot \tanh(kH) \tag{1}$$

Where $\omega = 2\pi f$ and f is the frequency, $k = \frac{2\pi}{\lambda}$ is the wavenumber.

The flexural modulus is expressed as the following (with E the Young modulus and ν the Poisson ratio) :

$$D = \frac{Eh^3}{12(1-\nu^2)} \tag{2}$$

In practice, we are interested in a regime in which the tension term is negligible. In that case, the remaining terms are the gravity term (in which appears g) and the flexion term (in which appears D). The ratio of these two terms defines a characteristic length. The characteristic wavelength, λ_D, also called flexural wavelength, or gravito-elastic wavelength, is the wavelength at which there is a transition between the gravity and flexural regime, and is defined as the following (using the fact that $\lambda_D = \frac{2\pi}{k_D}$) :

$$\begin{aligned} gk_D &\equiv \frac{D}{\rho}k_D^5 \\ k_D &= \left(\frac{\rho g}{D}\right)^{1/4} \\ \Rightarrow \lambda_D &= 2\pi \cdot \left(\frac{D}{\rho g}\right)^{1/4} \end{aligned} \tag{3}$$

Furthermore, it is useful to write the dispersion relation of purely flexural waves. This dispersion relation becomes :

$$\omega^2 = \frac{D}{\rho}k^5 \cdot \tanh(kH)$$

In the limit $kH >> 1$ (deep water) :

$$\omega^2 \approx \frac{D}{\rho}k^5 \tag{4}$$

In the limit $kH << 1$ (shallow water) :

$$\omega^2 \approx \frac{DH}{\rho}k^6$$

We will see that in our experimental setup, we have to keep the term $\tanh(kH)$.

2.2 Characteristic wavelengths in the experiment

In our experiments, we used 2 different materials as elastic sheet. We are going to compute an order of magnitude for the flexural wavelengths for both of them, in order to predict roughly which mechanisms will dominate for the propagation of hydroelastic waves in our experimental setup.

The ice sheet is the material of main interest. In this case, a lower bound for the flexural modulus D (D_{low}) is given roughly by considering that the Young modulus E = 9 GPa and that the thickness of the ice sheet is about 500 µm. An upper bound D_{up} is to consider the same Young modulus and a thickness of about 3 mm. The Poisson ratio of the ice is about 0.4 and its density about 10^3 kg $\cdot$ m^{-3}.

$$\begin{aligned} D_{low} &\approx 0.1 \text{ Pa} \cdot \text{m}^3 \\ \Rightarrow \lambda_D^{low} &\approx 0.36 \text{ m} = 36 \text{ cm} \\ \\ D_{up} &\approx 24 \text{ Pa} \cdot \text{m}^3 \\ \Rightarrow \lambda_D^{up} &\approx 1.4m \end{aligned} \tag{5}$$

The other material, commonly used in our experimental team, is a PDMS elastic film of 520 μm. Its Young modulus has been measured previously by our experimental team : $E = 1.6 \cdot 10^6$ Pa. However it may have changed over time. We can compute, for this elastic film, the corresponding flexural wavelength λ_D :

$$\begin{aligned} \lambda_D &\approx 4.0 \text{ cm} \\ \text{(Since we computed } D &\approx 1.6 \cdot 10^{-5}\text{Pa} \cdot \text{m}^3\text{, } \rho = 965kg \cdot m^{-3}\text{, and } \nu \approx 0.5\text{)} \end{aligned} \tag{6}$$

Looking at these characteristic wavelengths, we see that in the case of PDMS we might observe both gravity and flexural waves. However, for the ice sheet, we expect to be always in the elastic regime, because our experimental setup allows us to measure wavelengths of the order of 10 cm (maximum).

Therefore, if we are able to measure hydroelastic waves with our setup, we will expect to see only flexural waves. As the flexural regime is governed by the flexural modulus D, depending on ice proporties such as its thickness and its Young modulus. Therefore, we are quite satisfied to see that our experimental setup can, in principle allow us to measure such ice properties.

3 Numerical tools

Over the first weeks of this internship, we looked for an experimental technique to measure vertical displacement within the ice which are the order of 10 µm. We first tried to use a method called Synthetic Schlieren (method developped in 2009 [MRS09], that consists in placing a pattern below the water tank, and using the refraction of the rays to reconstruct the elevation of the surface). This method didn't work since the surface of the ice was too rough. We also tried to measure the deflection of a laser beam on the surface of ice. Eventually we found that the most reliable tehchnique was to used Particle Image Velocimetry (PIV), to measure the vertical velocity field of the ice sheet. This method is widely used usually to measure velocity fields in hydrodynamics, using tracer particles that are assumed to not change the properties of the fluid. However, in our case, we are dealing with a solid (the ice). Using the proper setup, the idea of the method we have developed is to track the local roughness of the surface of the ice sheet.

3.1 PIV (particle image velocimetry)

3.1.1 Explaination using synthetic images

The method we are using, mostly used in hydrodynamics in order to track the velocity of fluid particles, can be summarized using an example. The principle of this method is to cut images into small squares (also called "windows", or "boxes"). The algorithm measures the translation of the patterns inside the window at two successive times, using digital image correlation.

Let us use a simple python code to explain the process.

- Let us take an image with a random pattern on it (c.f. Image a on Fig.3). To do so, we have created a 2d array of shape 5×5 with random integer values for 0 to 3. We call it "image a", and it corresponds to the image at time t_0
- At time $t_0 + Dt$ we create an image that is the result of shifting up the image a by one pixel (c.f the top-right image of Fig.3). To do that, we have deleted the first row and added at the last row new random integer numbers, also distributed between 0 and 3.
- the cross-correlation between the 2 images is computed, here using the function correlate2d from the module scipy.signal (python) (c.f. the bottom color map on Fig.3). However the PIV algorithm that we use is implemented on matlab, even though the principle is the same.
- the position of the maximum of the cross-correlation is extracted, taking the pixel of the correlation with the maximal value. To improve the accuracy, the algorithm PIVlab (developed by William Thielicke : see articles [TS14] and [TS21]) that we use to analyse our images performs subpixelar detection by fitting the resulting correlation map with a Gaussian (in 2 dimensions).Thanks to this method, displacements, typically of the order of 0.1 pixels can be detected.

3.1.2 PIV algorithm in practice

Now that we have explained the basic idea of digital image correlation, we can explain the essential ideas of how the velocity fields are computed from a sequence of images by the PIVlab algorithm :

- First of all, we give, as an input parameter, the width W of the boxes, in pixels that are taken to compute local cross-correlations. The correlations are computed between boxes ("sub" images) separated by a time interval (in the unit of number of frames) Dt, which is the second input parameter that we have to enter.

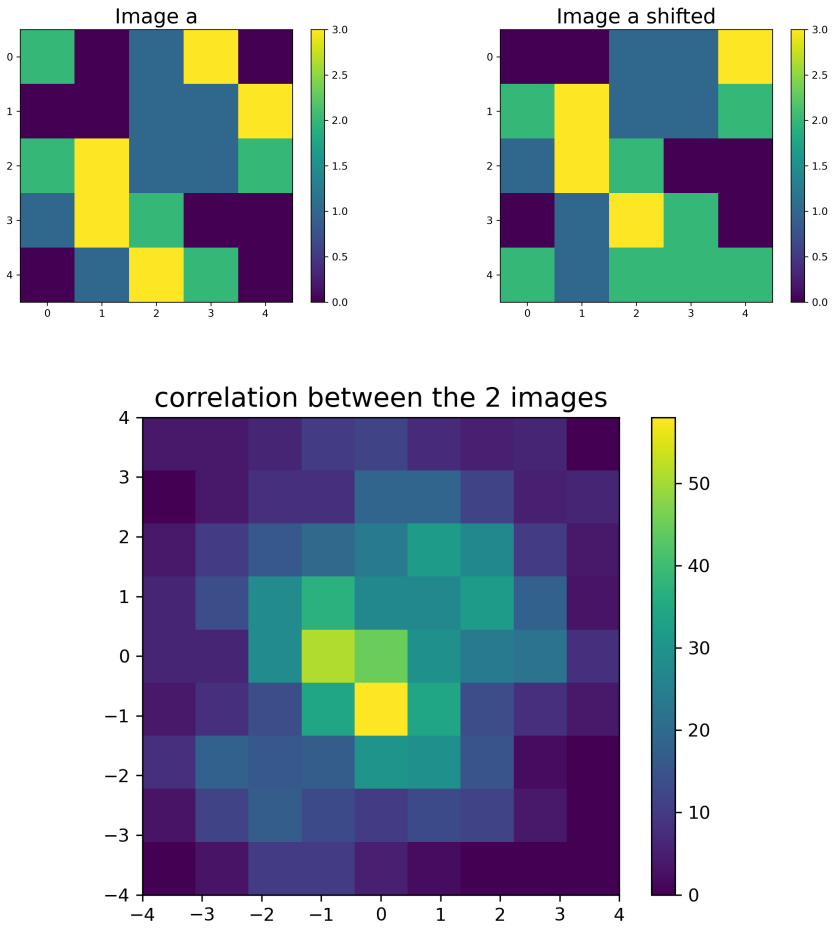

Figure 3: Illustration of the PIV method using synthetic images : we generated with a python code an image with 5×5 pixels using random numbers with 4 possible values (represented 4 different colors) (left) and the same image "shifted-up" by 1 pixel. The third figure (below) is the cross-correlation between the two images. The maximal value of this correlation map is the yellow pixel. It shows indeed a maximum of correlation for a vertical shift of one pixel

- At each time step, each box of size $W \times W$ is compared with the box at the same position on the image taken Dt frames before the current one. They are "compared" by computing their cross-correlation, as in the example given above (Fig.3).
- for each box position the (x,y) position of the maximum of correlation is extracted.
- converting Dt in seconds, and the pixels in meters, one can easily convert the maxima of correlation into a set of local velocities $(V_x(x, y, t), V_y(x, y, t))$.
- In the end the resolution that we get is "divided" by $\frac{W}{2}$ with respect to the image resolution, because the space interval between boxes is $\frac{W}{2}$ pixels.

3.1.3 Conversion of coordinates and distances from pixels to windows units

It is useful to write down how we change scales from an image to a PIV field. The formula to relate coordinates in pixels on the image to coordinates in PIV boxes (or "windows") is the following :

$$y_{pixels} = \frac{W}{2} + \frac{W}{2} \times y_{boxes} \tag{7}$$

Indeed, the PIV windows are of size W and separated by a half-window (size $\frac{W}{2}$), and we simply have to shift the origin when we change units so that the position of a PIV window is at the middle of it. However, one should not be confused, because the distance are still converted with the relation :

$$d_{pixels} = \frac{W}{2} \times d_{boxes} \tag{8}$$

3.1.4 Maximization of the PIV efficiency

Some remarks can be made concerning this algorithm : in some cases, increasing Dt can increase the accuracy significantly. For instance, when we excite the system with only a sinusoidal wave of one frequency, using stroboscopy allows to choose an optimal value for Dt, that maximizes the measured signal, which is useful in the case of our experimental setup, where the displacements of the ice are very small (comparable to the pixel size, or even smaller). We illustrate this in the figure 4 with synthetic data points.

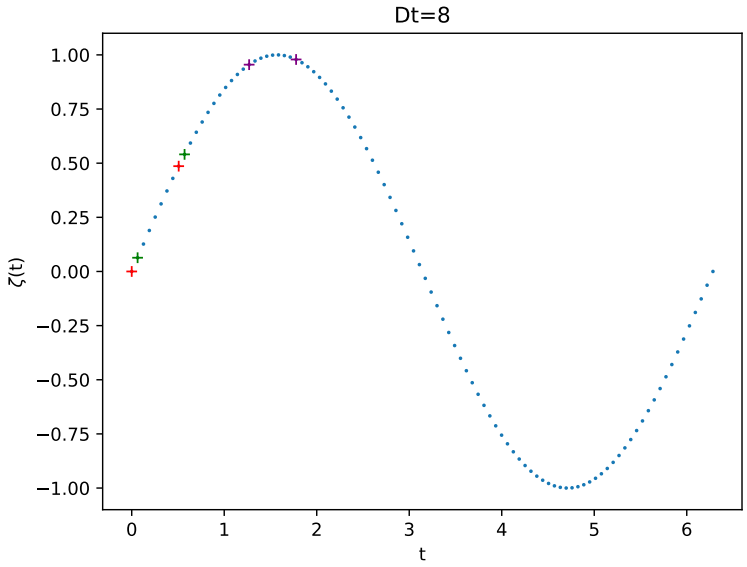

Figure 4: One period of a synthetic sinusoidal signal $\zeta(t)$, sampled with 100 (blue) points. For instance, when we choose $Dt = 8$, the value of ζ is compared between the two red crosses. At the successive time, ζ is compared between the two green crosses, etc. We show also 2 purple crosses, around a local maximum of the signal. This shows that this choice of Dt is still reasonable enough to approximate at linear order instantaneous velocities $\dot{\zeta}(t)$. However, taking a higher value for Dt will give less accurate values, but will increase the signal with respect to the noise, which can be interesting. We will see in a further analysis that we chose $Dt = 16$ as a good compromise.

Furthermore, if the signal is very noisy, it is also useful to increase the value of the box size W, because in this way the cross-correlation averages out the fluctuations. Of course, one must be careful that the value of W has to be small compared with the typical length of spatial variations of the velocity field, to ensure that the displacement is homogeneous within one box. We will see that it is indeed the case in our experiment with the ice sheet.

3.2 Fourier transforms

3.2.1 Continuous case

In the physics of waves, one useful tool is the Fourier transform, and, in practice, the algorithm of fast Fourier transform (FFT). In general, if we are interested in a system with small perturbations with respect to an equilibrium state, we can linearize it, and, since any potential can be approximated near

a local minimum by a quadratic potential, the corresponding solutions are sinusoidal functions, which are the Fourier modes.

For a 1-dimensional signal $\zeta(t)$, each Fourier mode is characterized by a frequency f, so that we can decompose $\zeta(t)$ in this basis, by summing the projections of $\zeta(t)$ on all these sinusoidal (Fourier) modes. We define the Fourier transform as the following (with $\omega = 2\pi f$):

$$\mathcal{F}(\zeta(t)) = \hat{\zeta}(\omega) = \int_{-\infty}^{\infty} e^{-i\omega t}\zeta(t)dt \tag{9}$$

And the inverse Fourier transform as :

$$\overline{\mathcal{F}}(\hat{\zeta}(\omega)) = \zeta(t) = \frac{1}{2\pi}\int_{-\infty}^{\infty} e^{i\omega t}\hat{\zeta}(\omega)d\omega \tag{10}$$

3.2.2 Discrete case

In practice, we look to discrete, and finite signals, with a sampling frequency (F_S, but also called f_{acq}), and size L. From the sampling frequency one can define the sampling time $T_S = \frac{1}{F_S}$, and therefore the values of time (taking as first instant $t_0 = 0$) will be a list with values : $[0, 1, 2, \ldots, L-2, L-1] * T_S$ (containing L values of times). The Fourier transform in this case, is a sum, instead of an integral, since we have a finite acquisition frequency.

The frequencies values at which can be evaluated the Fourier components are $[-\frac{L}{2}, -\frac{L}{2}+1, \ldots, \frac{L}{2}-2, \frac{L}{2}-1] * \frac{F_S}{L}$. Therefore the possible ω values are $[-\frac{L}{2}, -\frac{L}{2}+1, \ldots, \frac{L}{2}-2, \frac{L}{2}-1] * \frac{2\pi F_S}{L}$. The algorithm commonly used to compute discrete Fourier transforms is the algorithm of "Fast Fourier Transform" (FFT).

One main issue of the discrete Fourier transform is that it may lack of accuracy. A trick that is commonly used in order to artificially improve its resolution in frequency is the zero padding. It consists in adding the same number of zeros "at the left" and "at the right" of the signal. It permits to smooth the Fourier transform, which allows a better detection of peaks in the spectrum. We commonly choose the numbers of zeros such that the total number of points ($= L$) is a power of 2, which optimizes the efficiency of the FFT algorithm.

3.2.3 The use of Fourier transforms for wave dispersion relations

Here, we illustrate how useful are Fourier transforms to measure how waves propagate in a system. The way waves propagate in a system is summarized in an expression called the dispersion relation. This relation expresses the wavenumber (or analogously the wavelength) to the frequency of the wave. Since the phase velocity of a sinusoidal wave of a given frequency is related to both the frequency and the wavelength, this relation can also be seen as the speed of the wave as a function of the frequency of the wave.

To illustrate how to use Fourier transforms (and in practice FFT) in order to get a dispersion relation, we start by the following :

- We create a sinusoidal spatio-temporal signal $\zeta(x, t)$ of size $L_X \times L_T$. We show this signal on a spatio-temporal diagram (Fig.5), where the color scale gives the value of ζ.
- We show the magnitude of its 2-dimenstional Fourier transform, computed with the algorithm FFT2 on Fig.6. We observe that each couple (k,f) will give a single point on the Fourier transform in general.

In order to get a dispersion relation, we need to measure f vs k for many values of f. Therefore, we introduce a common way to measure a dispersion relation using FFT in any system. We know that every signal can be decomposed into a sum of Fourier modes with many frequencies. The signal that contains an infinite amount of frequency and for which each Fourier components are equal is the Dirac delta $\delta(t)$. In theory, it is therefore convenient to use such signal to excite a system, so that we see in the best possible way which couples (k,f) are selected by the system, giving rise to a dispersion relation. Since the Dirac delta has a vanishing width, it is not possible to impose such a function experimentally to any system. To approach at least this idea, we apply a pulse of finite width, which contains a continuum of frequencies in a relatively broad range. For instance, in the case of a softer material than the ice, like a PDMS elastic membrane, as we used to test our experimental setup, we managed to get a dispersion relation for frequencies ranging from 0 to 70 Hz.

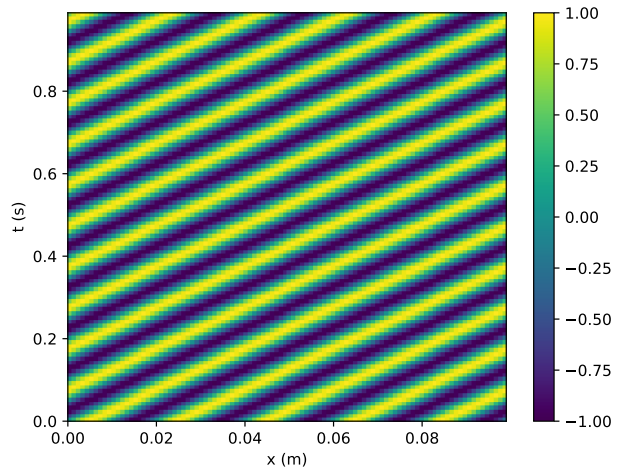

Figure 5: Spatio-temporal diagram of an artificial sinusoidal signal, with frequency $f = 10$ Hz and wavelength $\lambda = 2$ cm.

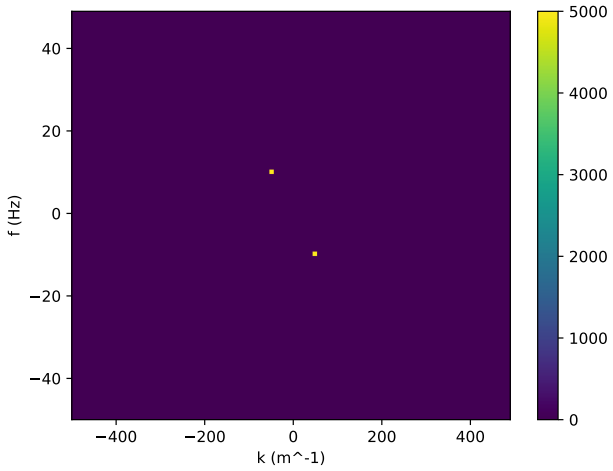

Figure 6: Magnitude of the 2D-Fourier transform of the spatio-temporal signal from figure 5. We see two peaks exactly at the frequency and the wavenumber at which we generate the artificial wave. The fact that there are two peaks instead of one is explained by the fact that we can see the diagram from Fig.5 as a wave propagating backward for increasing times, or as a wave propagating forward for decreasing times.

3.3 A combination of stroboscopic measurements and Fourier analysis

3.3.1 Stroboscopy

In our experiments, due to technical limitations, the waves that we produce have wavelengths of the order of the system size. If we want to measure accurately enough the wavelength for each frequency, or equivalently the phase velocity, we need to impose pretty high frequencies to the ice surface (our system size is of the order of 30 cm, and the waves that we have to apply to see enough spatial variation in the velocity field must have frequencies of at least 30 Hz). Since the acquisition rate of the camera is limited to about 200 Hz, it is convenient to use stroboscopy, so that we can make measurements at higher frequencies. Here we are going to explain the principle of this method.

In general, stroboscopic measurements turn out to be very efficient whenever the signal that we want to analyse is periodic, and that we know this period. In the physics of waves, when we impose to

a system a sinusoidal forcing at a frequency f_{exc}, we expect from it to respond at the same frequency. Therefore, in our case, where a wave maker is generating sinusoidal waves on the surface of ice, we employ such measurements. The main interests of performing stroboscopic measurements is that we can overcome technical issues due to a potential limited sampling rate. Furthermore, we will see that time resolution is particularly important for our experiment, because, instead of measuring wavelengths, we will measure phase velocities, which involves both time and space. Therefore, we explain in this part how we have put in practice this method.

We proceeded as the following. Let us call $T_{exc} = \frac{1}{f_{exc}}$ the period of excitation. If we want to sample one period with 100 points, separated by a $\Delta t_{sample} = \frac{T_{exc}}{100}$, we need the acquisition period T_{acq} to be equal to an integer number of periods *plus* Δt_{sample} :

$$T_{acq} = N \times T_{exc} + \Delta t_{sample} \tag{11}$$

Of course, since the signal is never perfectly periodic, the smallest is N, the better it is. Therefore, in many cases, we will take $N = 1$, i.e. $T_{acq} = T_{exc} + \Delta t_{sample}$, but, since sometimes f_{exc} is higher than the highest possible frame rate f_{thr}, we take a bigger value for N (2, 3...). To compute the acquisition frame rate f_{acq}, we calculate $f_{acq} = \frac{1}{T_{acq}}$, choosing the smallest possible value of N and then checking that $f_{acq} < f_{thr}$. Applying this method, no matter how big is f_{exc}, two consecutive frames will be always separated by the same fraction of period $\frac{\Delta t_{sample}}{T}$.

3.3.2 How to extract quickly the component of the signal at a given frequency

Let us again consider our signal $\zeta(t)$, from which we want to extract the component at the frequency f_{exc}. As above, we start with the definition of the Fourier transform :

$$\hat{\zeta}(f) = \int_{-\infty}^{\infty} e^{-2i\pi ft} \zeta(t) \cdot dt \tag{12}$$

The component of the field at the frequency f_{exc} is the inverse Fourier transform of a Dirac delta $\delta(f - f_{exc})$ multiplied by $\hat{\zeta}(f)$:

$$\begin{aligned} \zeta_{f_{exc}}(t) &= \frac{1}{2\pi} \int_{-\infty}^{\infty} e^{2i\pi ft} \hat{\zeta}(f) \cdot \delta(f - f_{exc}) \cdot (2\pi df) \\ &= e^{2i\pi f_{exc} t} \int_{-\infty}^{\infty} e^{-2i\pi f_{exc} t'} \zeta(t') \cdot dt' \end{aligned} \tag{13}$$

In practice, we use a discrete sum over the entire time series. Note that $\zeta_{f_{exc}}(t)$ is a complex number with an amplitude A equal to the modulus of the Fourier transform evaluated at the frequency f_{exc}, and a phase factor equal to $\frac{\zeta_{f_{exc}}(t)}{A}$. In order to visualize the filtered signal as a function of time, one can plot the real part of this complex number, $\mathcal{R}(\zeta_{f_{exc}}(t))$. And we will see later that it is convenient to plot the real part of the phase factor when we are only interested in the spatio-temporal variation of the phase for instance.

In our analyses, we will have sequences (evolution in time) of PIV fields (matrices). Therefore, the temporal evolution of some matrix element can be seen as a 1-dimensional signal (like $\zeta(t)$). The result of the operations given above give a matrix of complex numbers. We will call that matrix the complex field.

3.3.3 Combination of the two methods

In both methods that we have just discussed, we are interested in how a physical system behaves, excited at a given frequency f_{exc}. To use stroboscopic measurements and Fourier analysis at the same time, we proceed as the following :

- we choose the acquisition frequency f_{acq} such that we sample a full period of the signal with 100 points, and record our data in that way.
- if we recorded 1 period, our data set contains 100 data points. Therefore the list of time values at which the signal $\zeta(t)$ is evaluated is : $\frac{1}{f_{acq}} \cdot [0, 1, 2, \ldots, 99] = T_{acq} \cdot [0, 1, 2, \ldots, 99]$. In the following, the i^{th} element of this list will be denoted t_i.

- we compute the sum : $\sum_{i=0}^{99} e^{-2i\pi f_{exc} t_i} \zeta(t_i) \cdot \Delta t_{sample}$ (discrete sum over the entire time series).
- we get eventually : $\zeta_{f_{exc}}(t_i)$ by multiplying this sum by $e^{2i\pi f_{exc} t_i}$, and we can visualize it in real space by taking its real part.

Thanks to this protocol, we can isolate and visualize the propagation of the monochromatic wave excited in the thin sheet.

4 Experiments

4.1 Experimental setup

The experimental setup is the following : we put a transparent water tank of dimensions 50 cm×60 cm in a refrigerator. We can pass the necessary electrical connections through a small hole on the side of the refrigerator. The tank is filled with distilled water (to avoid mineral depositions) with a depth of about 3 cm. The tank is not in contact with any metallic pieces, because their high thermal conductivity induces strong heat flux in some precise zones, that we want to avoid. Indeed, we want to make freeze the ice only by thermal transfers from the air of the fridge to the water surface to get the most homogeneous ice possible. In order to isolate the system from other heat source than the air in the fridge, polystyrene plates have been disposed on the sides of the tank. Four ventilators have been placed in order to increase thermal exchanges between air and the water surface. A metallic rod is screwed on the vibration exciter, and on the edge touching the water surface is added a circular piece of tissue in order to maximize the coupling between the vibration exciter and the ice (the whole tissue is stuck inside the ice when it has frozen), and prevent neighbouring ice to break too easily. In order to capture the vertical component of the local motion of the ice sheet, a digital camera is making acquisitions from outside of the fridge, with a quite small angle (between 10 and 15 degrees) with respect to the water surface.

One our experiment has been set up, to prepare the acquisitions, we proceed as follows :

- We put a water in the tank (a depth of about 3 cm)
- We turn on the refrigerator and all the ventilators, and wait about 5 hours for the surface of water to freeze
- The air inside the fridge reaches a temperature between -5°C and -2°C and there is a thickness of ice between 0.5 and 3 mm.
- We perform acquisitions in order to extract the phase velocity for various frequencies
- We measure the thickness of ice, either using a caliper, or measuring the weight and the surface of some part of the ice sheet that we have carefully removed from the surface of water.

Many experiments, and experimental configurations have been tested during this internship (camera above, camera on the side, camera inside of the refrigerator, camera outside of the refrigerator, light coming from below/above/side...). In this report we only discuss one configuration, where the camera is recording images of the surface from the side, with an inclination angle between 10 and 15 degrees. For the first data set we discuss, the inclination angle of the camera is 14° and the light comes from the side. We show an image from one of the sequences taken in that configuration, where the ice surface is excited with the frequency $f_{exc} = 100$ Hz and the camera is taking acquisitions with the frame rate $f_{acq} = 99$ Hz.

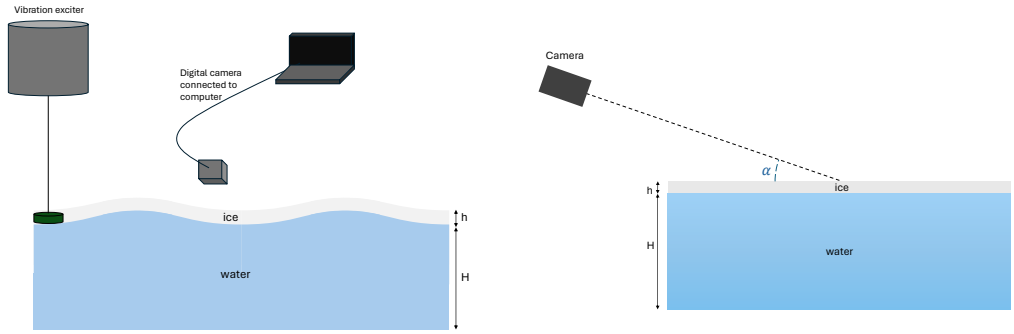

Figure 7: Sketches of the experimental setup. On the left we sketched the wave propagation in the plane of observation, and a digital camera making acquisitions. On the right we show the inclination of the camera, making an angle α with respect to the ice surface

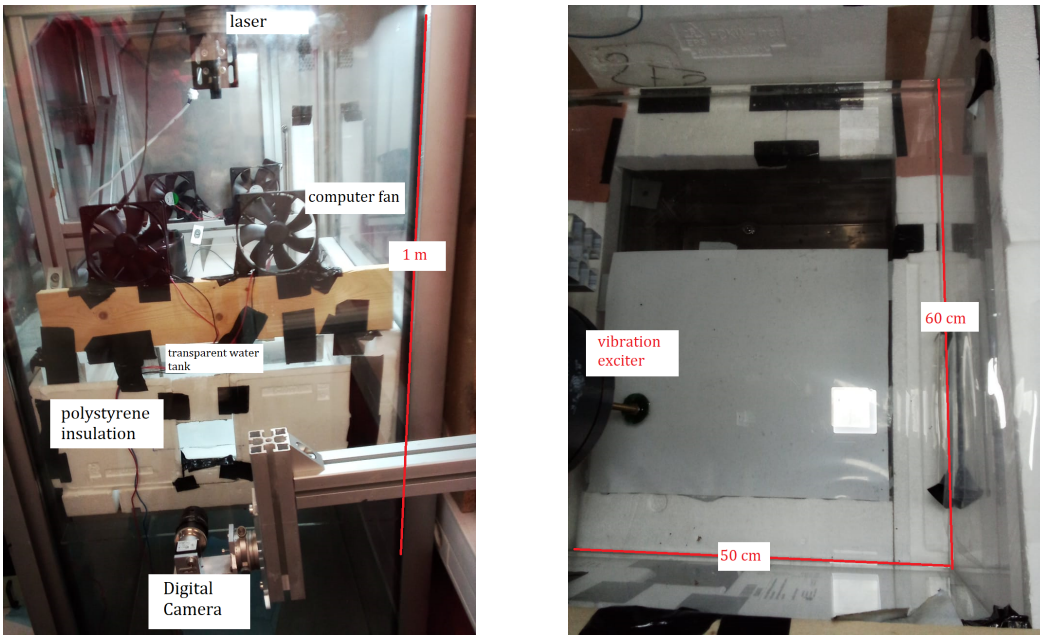

Figure 8: Photography of the experimental setup : view from outside of the refrigerator (left) and view from above inside of the refrigerator (right)

4.2 Testing the experimental setup with a known material

We tested the experimental setup, as described in Fig.8 with a material well known for its elastic properties and that have been studied already in our experimental team previously [Dom18]. The membrane of PDMS that we have used has a thickness of $520\mu m$. Its Young modulus is $E = 1.6$ MPa. Its density is $\rho = 965$ kg·m^{-3}.

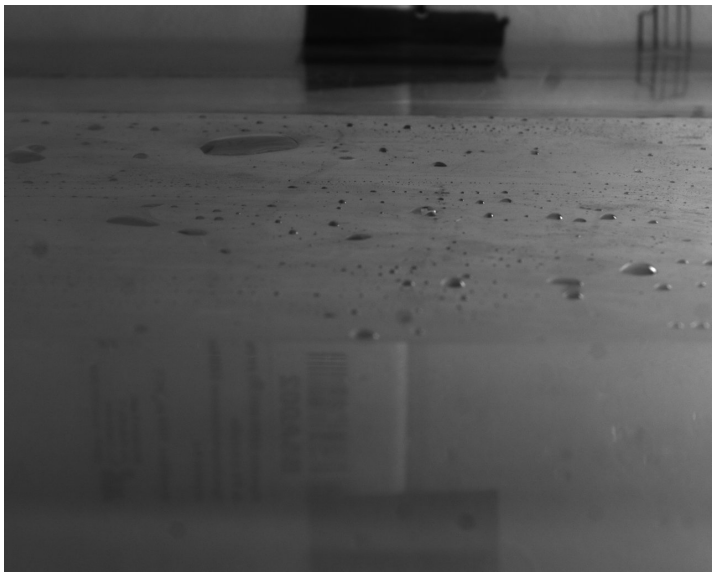

Figure 9: Picture of a floating elastic PDMS membrane, taken from the sequence of images in which we apply a pulse to its surface. We voluntarily added droplets on the surface of the membrane to add texture, for PIV analysis.

The goal of this experiment was to get the dispersion relation of hydroelastic waves in the PDMS membrane, with the same experimental setup that we have used for the ice. In order to get the dispersion relation of the membrane, a pulse has been applied on it, creating a radial wave packet with a wide range of frequencies. Choosing a profile line on the images in order to get a space-time signal (with one dimension for space, and one dimension for time) , and computing its 2D - Fourier transform, we get the figure (10), by taking the modulus of each element of the resulting 2D array. On this figure, the color code is the magnitude of the Fourier mode as function of k and f. The experiment is reasonably in agreement with the theory. This validates our experimental setup, and therefore we can use it for real ice.

To conclude about the experiment on the membrane, we are satisfied with the validation of our experimental technique, that we will use to measure waves in the ice. However, in the case of the membrane, the FFT method works well because the wavelengths are small enough. It will be a bigger problem in ice, since in that case we expect that the wavelengths will be of the order of the system size. So we will move to real space and look directly at the phase velocity. We will use the fact that, for a monochomatic wave, the phase velocity is related to the wavelength, since $v_\phi = \frac{\omega}{k}$. Therefore, with this method we will be able to measure the wavelengths indirectly, "at the sub-wavelength scale".

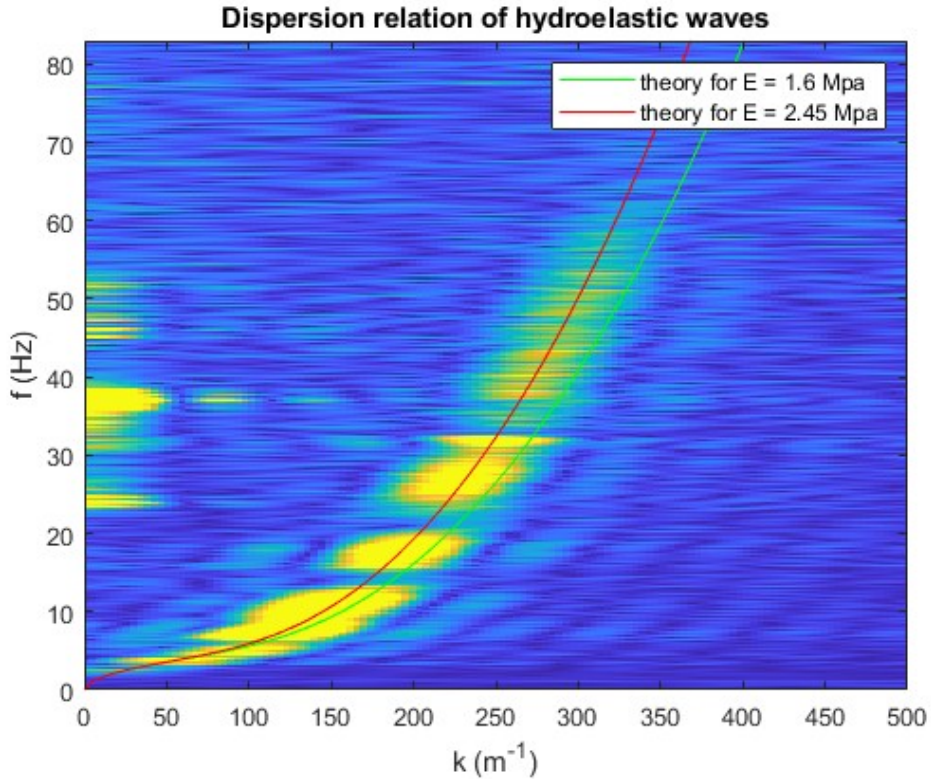

Figure 10: Dispersion relation in the PDMS membrane, computed by taking the modulus of each metricial element of the 2D-FFT of the spatio-temporal signal. In other words, this figure is the measure of the intensity of waves, as a function of the spatial periodicity (in m^{-1}) and the temporal periodicity (in Hz). The theory of hydroelastic waves in this specific case is plotted in two cases : for E=1.6 Mpa, and E=2.45 MPa. The theory seems to fit more with the theory for E=2.45 MPa. We remark some peaks of amplitude of the Fourier transform that do not correspond to the theory, for instance around $f = 38$ Hz. These peaks are due to a global motion of the camera for some specific frequencies, and are therefore disregarded.

4.3 A first experiment to put in evidence ice heterogeneity

In this first experiment, we apply the procedure that we described in 4.1 to show that local information can be extracted even when the ice contains heterogeneities. We use a technique, that is measuring the phase velocity instead of the wavelength, to improve spatial resolution.

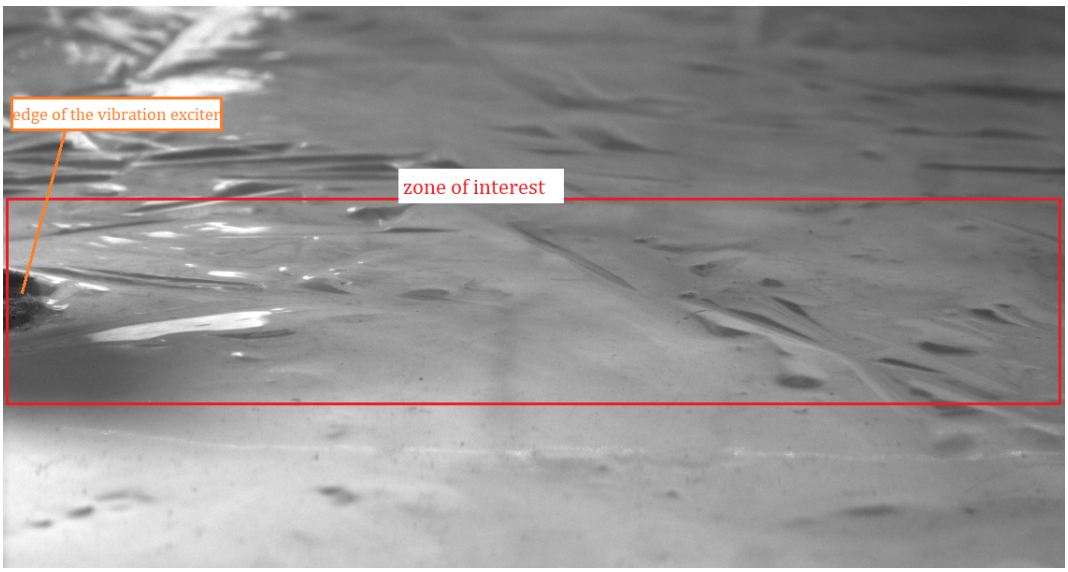

Figure 11: Picture of ice grown in the lab. We observe a very heterogeneous surface. In particular, we see an important defect at the center of the image that might separate two regions with different properties. The zone that will be of interest will be the central region, and in particular the horizontal profile in the continuity of the wave maker that we can see on the left. This image comes from a data set with $f_{exc} = 100$ Hz and $f_{acq} = 99$ Hz

We can see on this image that the ice displays a lot of heterogeneities. Moreover, we see that a considerable part of the ice surface is blur, and therefore the velocities measured by the PIV algorithm might lack of accuracy in these regions. For this data set, we use for all frequencies : $W = 32$ and $Dt = 8$. We remind that, increasing the value of Dt increases the signal that is measured, which is good since the displacements are very small. We use these parameters to run the PIV algorithm, and we extract the component of the vertical velocity field V_y (signal of interest). We show (Fig.12) the phase of the component of the field at 100 Hz of the signal, at two different times (t_0 and $t_0 + \frac{T}{2}$).

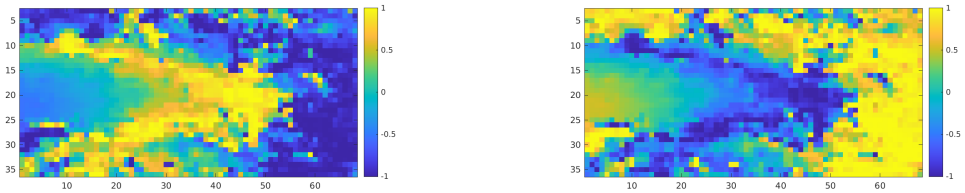

Figure 12: Real part of the phase factor $\mathcal{R}(e^{2\pi i f t + \phi(x)})$ of the field at a time t_0 (left) and a time $t_0 + \frac{T}{2}$ (right), for the excitation frequency of 100 Hz, taken from the data set 20240523. On these 2 figures, we see that the wave maker is producing circular propagative waves. Between the two images, the wave front seems to have moved about the half of a wavelength.

The next step is to plot a space-time diagram in order to visualize the wave propagating along a chosen profile. For this data set, we use the profile line along the 17^{th} row ($y = 16$) of the component

f_{exc} of the signal.

First of all, we show (Fig.13) the raw PIV field V_y at vertical position $y = 16$. In this case, we see 2

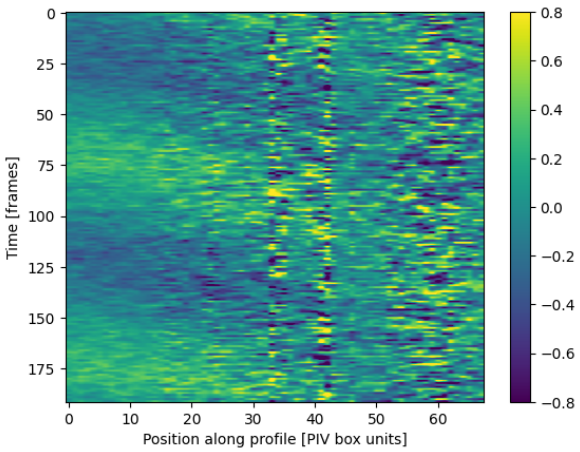

Figure 13: Spatio-temporal diagram given by the raw PIV data, showing 2 periods. We can see the wave propagating in the left part of this diagram, while the right part is very noisy

time periods, which was indeed expected because we recorded 200 frames and each period is sampled with 100 points. One can see a wave propagating in the left part of this diagram, while the right part is very noisy. Projecting on a single Fourier component, as on Fig.14 improves the resolution.

We proceed as the following : We show the space-time diagram, that we constructed by creating 3 periods of "artificial times" by putting 256 points in one time-period and computing for each row (time index i) of the matrix the profile at the corresponding time. We remark that we can show directly the matrix which elements are the displacements (in pixels) computed during the PIV procedure. In this way we can see in which regions the displacements are of higher amplitude. Then, if we want to visualize better the propagation along the whole profile, we can plot the evolution of the real part of the phase factor. Furthermore, since, for some frequencies, the data is too noisy, we smooth spatially the 1-dimensional profile at each time step, using the function savgol_filter from the module scipy.signal in python (setting the window size to 21 and the order to 3). Here is an illustration of this step :

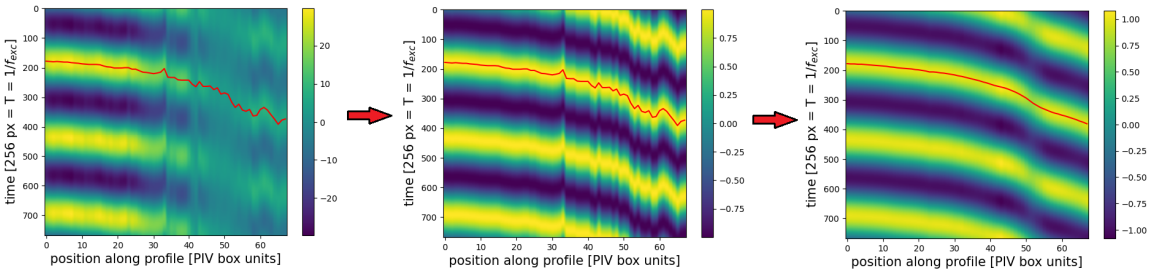

Figure 14: 3 space-time diagrams at vertical position $y = 16$, represented in 3 different ways. The first one (left) shows the real part of the profile extracted at the frequency 100 Hz at different times. We can see that, along its propagation, the signal decreases its amplitude. As we are interested in the local velocity, we normalize the signal at each position by its modulus to obtain the second figure (middle). This second figure is the real part of the phase factor as a function of space and time. Because of the ice heterogeneity, noise appears in the second diagram. We smooth each row of the second matrix to obtain the third diagram (right).

Next, we fit the detected wavefront (red line on the figure 14) with a linear function, once time and space converted into physical units. The phase velocity is, by definition, the speed of this wavefront, and therefore the slope given by the fit. To conclude about these measurements : when the ice is very heterogeneous, we can think of a method that takes advantage of the spatial variations of the phase

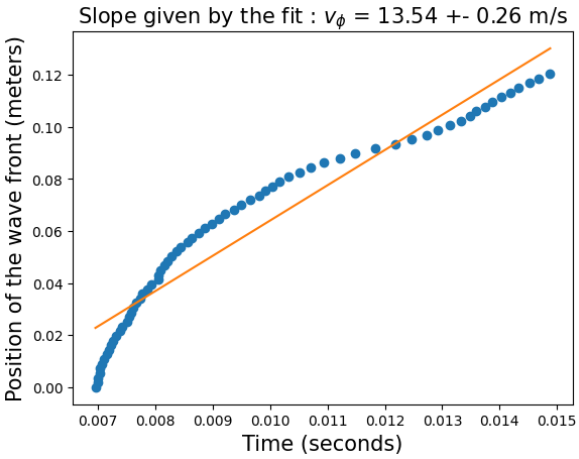

Figure 15: Linear fit of the position x of the wavefront (in meters) as a function of time (in seconds). The slope depends on time, that indicates that the wave is faster in the left region (from 0 m to 0.06 m) than in the right region (from 0.06 m to 0.12 m). Therefore, the fit gives only an estimation of the average phase velocity. To go further, and better probe locally the ice properties, the idea would be to make two different linear fits, in the two distinct regions.

velocity in order to reconstruct a map of flexural moduli on an ice surface. Using our specific method would be even more interesting, due to the fact that tracking the velocity of a wave front can be made at the sub-wavelength scale. Therefore, the spatial resolution of the flexural modulus map, that we can make on a surface with this method, is increased with respect to a method that would use spatial FFT.

4.4 A second data set on ice to measure a dispersion relation

This last data set that we discuss is the one with which we got the main result of the internship, i.e. the dispersion relation of our ice sheet covering the surface of water. This data set contains several sequences of images, each one corresponding to a frequency of excitation. In the following parts, we explain in details how we obtain from one sequence of images, corresponding to one frequency, the corresponding phase velocity. For each sequence we will get one data point. The final result, that is the phase velocity as a function of the frequency will be given in the last part. Note that it has been processed in a very similar way than the first data set.

4.4.1 Set up

We grow an ice sheet of (1.5±0.5) mm with our cooling method discussed in 4.1. PIV analyses require good contrasts to detect well spatial shifts. In order to increase the contrasts on the ice, we add pepper, that has been previously cooled down at the ice temperature, on the surface.

To illustrate, let us take an image from one of the sequences that we have recorded. Here for instance we chose the excitation frequency f_{exc} of 80 Hz, and the acquisition frequency f_{acq} is 79.2 Hz.

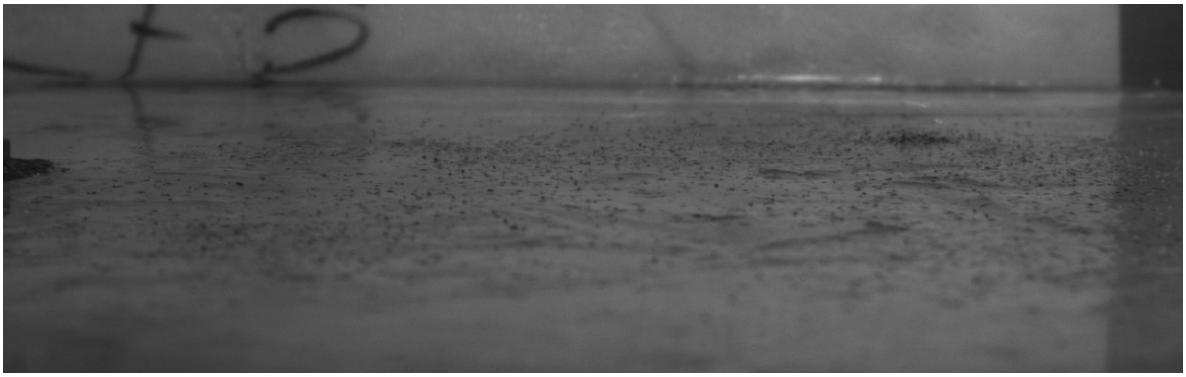

Figure 16: Picture of ice grown in the lab, with pepper on its surface to increase contrasts. We can see the edge of the wave maker on the left. This image belongs to the data set for $f_{exc} = 80$ Hz and $f_{acq} = 79.2$ Hz

4.4.2 Measure of the horizontal aspect ratio as a function of the position on the image

Because of the inclination of the camera, we must measure how changes the conversion of horizontal distances from pixels to meters as a function of the position on the images. To do so, we use the software ImageJ : we measure the distance dpx in pixels corresponding to a distance dcm in cm. In this way we can convert the vertical position of the profile line on which we want to see the wave propagating.

In order to set, not only a scale on one profile line, but to quantify how much does change the ratio $\frac{dcm}{dpx}$ as function of the vertical position on the image, we measured the ratio $\frac{dcm}{dpx}$ again with imageJ, for 3 different vertical positions and fitted with a line (see Fig.17) in order to get the horizontal aspect ratio for any point on the ice.

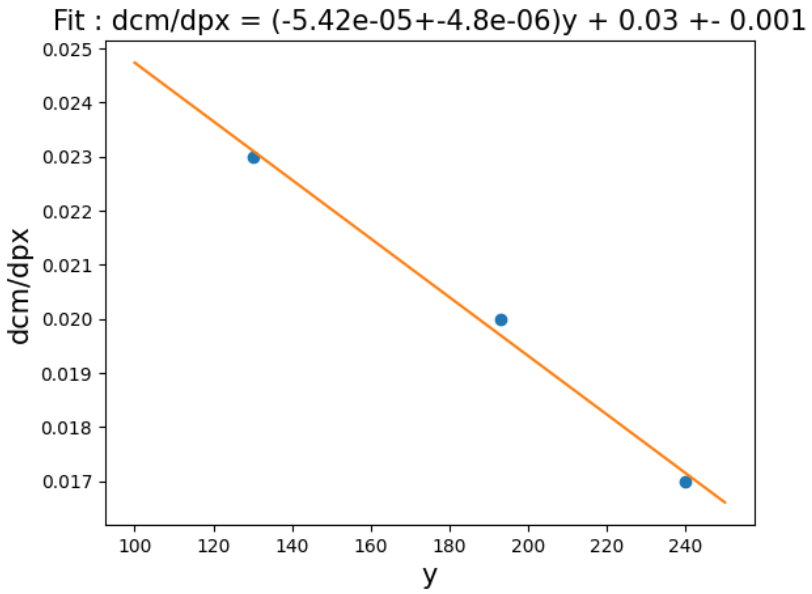

Figure 17: Fit of the ratio $\frac{dcm}{dpx}$ measured for 3 different positions on the y-axis, for the camera with an inclination angle of 10.5°, as in the 2nd experiment

4.4.3 PIV analysis, and filtering of the data

We processed the sequences of images with the PIV algorithm, with input parameters : $W = 64$ and $Dt = 16$.Then, from the PIV field, we extract the component of the vertical velocity field V_y. Afterwords, we extract the component of the signal at the frequency f_{exc}. We show, as an example, the real part of the phase factor at 2 different times. One time, arbitrarily called t_0, and a further time $t_0 + \frac{T}{2}$, where $T = \frac{1}{f_{exc}}$.

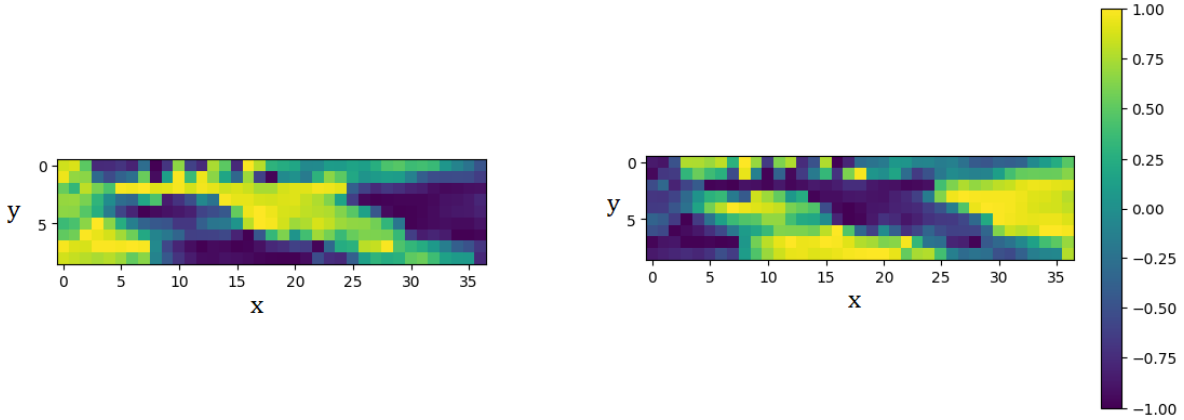

Figure 18: Real part of the field V_y extracted at the frequency $f_{exc} = 80$ Hz, at a time t_0 and a time $t_0 + \frac{T}{2}$, for the excitation frequency of 100 Hz, taken from the data set 20250604. We see two wave fronts that have moved on a distance of a half wavelength during a time $\frac{T}{2}$. The only relevant domain of these fields is for y ∈ [2,6], since it correspond to coordinates on the images where there is ice and it is not blur.

Making the assumption that, in the domain y ∈ [2,6], the wave is a plane and propagating in the x-direction we can compute its phase velocity by fitting a spatio-temporal diagram with a linear function, having converted time and space in physical units (where distances are converted using Fig.17. In the example of excitation frequency of 80 Hz, we show the spatio-temporal diagram of the profile at y=4. We show the fit of one of the maxima on the spatio-temporal diagram, after having smoothed out the profile at each time, using the Savitzky-Golay algorithm implemented in the module signal from the library scipy in Python (as input parameters we used : window size = 21, and order = 3).

On all the datasets, the range on which we fit is for x ∈ [10,33] (positions in PIV windows units: c.f. Fig.19). We remark how powerful is the PIV algorithm we are using, combined with our stroboscopic method, since the displacements measured are of the order of 10^{-1} pixels/(16 frames) $\approx 6 \cdot 10^{-3}$ px/frame. One can also get an order of magnitude for the amplitude of the elevation : $\frac{100}{4} \times 6 \cdot 10^{-3} = 0.15$ px. Converted in physical units : $2 \cdot 10^{-2} \times 0.15 \cdot 10^{-2} = 3 \cdot 10^{-5}$ m. We are able to measure waves of amplitudes of about ten microns !

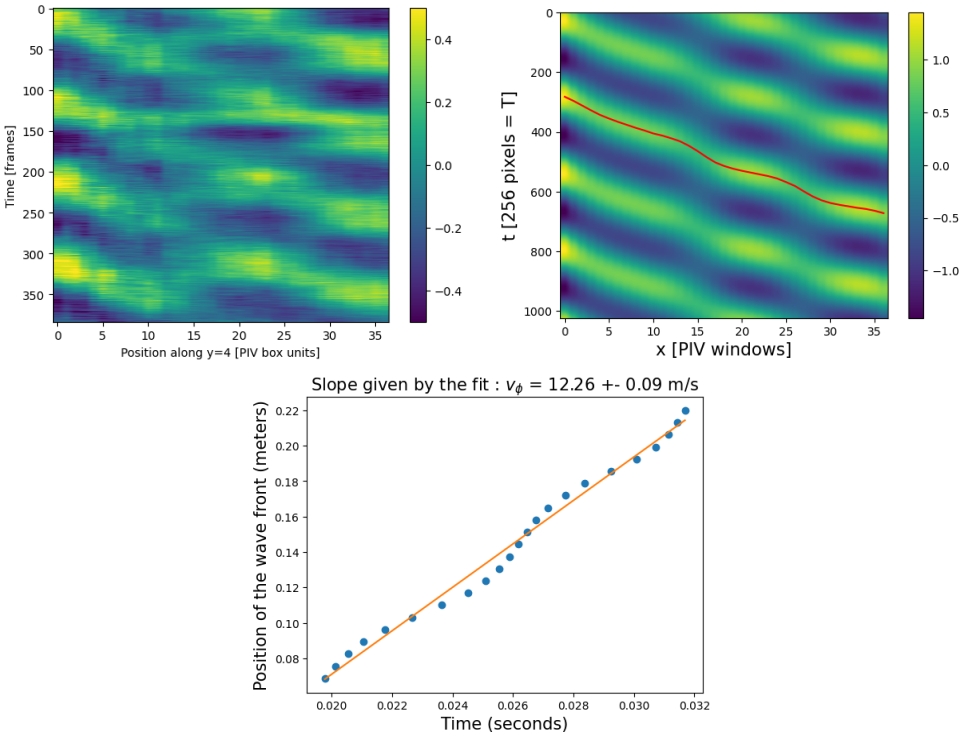

Figure 19: Spatio-temporal diagram using directly the raw PIV field (top-left). This RAW field is useful to compute the order of magnitudes of vertical displacements of the ice. The top-right diagram is the smoothed spatio-temporal diagram of the phase $\mathcal{R}(e^{2\pi i f t + \phi(x)})$. The red curve is a detected local maximum. The bottom plot is the linear fit of the detected position (in meters) of the local maximum as function time (in seconds). The slope of this fit is thephase velocity v_ϕ of the wave

4.4.4 Resulting dispersion relation

After having processed all the sequences of images with the routine discussed in the previous part, we are finally able to make a plot of the phase velocity measured experimentally as a function of the excitation frequency.

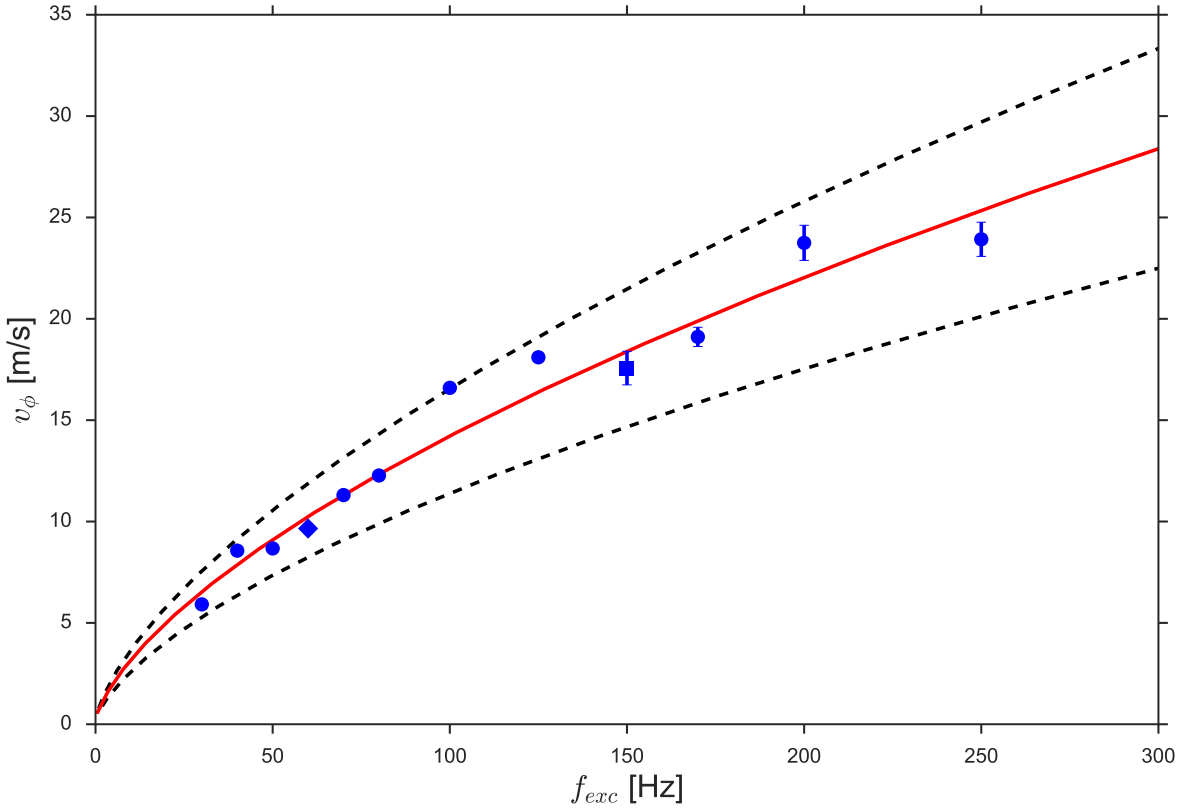

Figure 20: Dispersion relation of hydroelastic waves in the ice sheet, from the dataset 20240604. The theory (in red) have been computed for E=9 GPa and h=1.5 mm. The dotted black lines correspond to the theory for the same Young modulus and h=2mm for the upper line and h=1mm for the lower line. All the theoretical curves have been computed with zero tension : $T = 0$. All points belong to the same data set. The circles have all been got by processing the sequences of images exactly in the same way than the sequence for $f_{exc} = 80$ Hz. However, 2 data points were post processed in a slighly different way, because there PIV field were too noisy on the profile line $y = 4$. For $f_{exc} = 60$ Hz, we took the profile line $y = 6$. For $f_{exc} = 150$ Hz, we took the profile line $y = 5$. We used the fit (from Fig.17) to get the correct horizontal aspect ratio for each of them. The assumption that $T = 0$ seems to be in agreement with the experiment. All data points are situated in the flexural regime, because the theory predicts a cutoff frequency between the gravity and the flexural regime of about $f_{cutoff} = 0.3$ Hz.

5 Conclusion

During this internship, we built an analogous lab experiment to the sea ice such as in the Arctic ocean. Growing a very thin ice sheet, of a thickness of about 1 mm, with few defects, has been very difficult. Performing displacement measurements with an accuracy of about 10 µm was also particularly challenging. In the end, we managed to get a dispersion relation of waves in an ice sheet grown in the lab, that was in agreement with the theory of hydroelastic waves, and particularly in the flexural regime. This first result is promising, and we are looking forward to continue experiments with real ice in the lab, in particular to study the fracture mechanisms. We have put in evidence ice heterogeneity for a particular ice sheet that we grew, by observing different phase velocities in two different regions. To go further, we proposed the idea to measure local dispersion relations to draw a spatial flexural modulus map of the ice.

References

[Dom18] Lucie Domino. *Contrôle et manipulation d'ondes hydroélastiques*. PhD thesis, Université Paris sciences et lettres, 2018.

[MRS09] Frédéric Moisy, Marc Rabaud, and Kévin Salsac. A synthetic schlieren method for the measurement of the topography of a liquid interface. *Experiments in Fluids*, 46:1021–1036, 06 2009.

[SEP98] Peter J. Stein, Steven E. Euerle, and James C. Parinella. Inversion of pack ice elastic wave data to obtain ice physical properties. *Journal of Geophysical Research: Oceans*, 103(C10):21783–21793, 1998.

[TS14] William Thielicke and E J Stamhuis. Pivlab – towards user-friendly, affordable and accurate digital particle image velocimetry in matlab. *Journal of Open Research Software*, 2, 10 2014.

[TS21] William Thielicke and Rene Sonntag. Particle image velocimetry for matlab: Accuracy and enhanced algorithms in pivlab. *Journal of Open Research Software*, 9, 05 2021.

[TTN06] Takenobu Toyota, Shinya Takatsuji, and Masashige Nakayama. Characteristics of sea ice floe size distribution in the seasonal ice zone. *Geophysical Research Letters*, 33:L02616, jan 2006.

6 Appendix

6.1 Code for Fig.5

```python
import numpy as np
import matplotlib.pyplot as plt

delta_x_sample = 1e-3
fx = 1/delta_x_sample
x = np.arange(0,1e-1,delta_x_sample)
delta_t_sample = 1e-2
ft = 1/delta_t_sample
t = np.arange(0,1,delta_t_sample)
xx,tt = np.meshgrid(x,t)
lbd = 2e-2
k = 2*np.pi/lbd
freq = 10 #Hz
signal = np.sin(k*xx-2*np.pi*freq*tt)
plt.figure()
plt.imshow(signal,extent=[np.min(x),np.max(x),np.max(t),np.min(t)],aspect='auto')
plt.ylim(np.min(t),np.max(t))
plt.xlabel('x (m)')
plt.ylabel('t (s)')
plt.colorbar()
plt.savefig('artificial_signal.pdf')
plt.show()
tab_freq = np.fft.fftfreq(len(t),d=delta_t_sample)
tab_k = np.fft.fftfreq(len(x),d=delta_x_sample)
FT2 = np.fft.fft2(signal)
print(-np.pi/len(x),np.pi/len(x)-np.pi/(len(x)**2))
plt.figure()
plt.imshow(np.fft.fftshift(np.abs(FT2)),extent=[np.min(tab_k),np.max(tab_k),np.max(tab_freq),np.min(tab_freq)],aspect='auto')
plt.ylim(np.min(tab_freq),np.max(tab_freq))
plt.xlabel('k (m^-1)')
plt.ylabel('f (Hz)')
plt.colorbar()
plt.savefig('fft2_artificial_signal.pdf')
plt.show()
```